DIGITAL ACCESS TO SCHOLARSHIP AT HARVARD
DASH.HARVARD.EDU

HARVARD LIBRARY

Flow Batteries: Alkaline Benzoquinone Aqueous Flow Battery for Large-Scale Storage of Electrical Energy

Citation

Yang, Zhengjin, Liuchuan Tong, Daniel P. Tabor, Eugene S. Beh, Marc-Antoni Goulet, Diana De Porcellinis, Alán Aspuru-Guzik, Roy G. Gordon, and Michael J. Aziz. 2018. “Flow Batteries: Alkaline Benzoquinone Aqueous Flow Battery for Large-Scale Storage of Electrical Energy (Adv. Energy Mater. 8/2018).” Advanced Energy Materials 8 (8) (March): 1870034. doi:10.1002/aenm.201870034.

Published version

https://doi.org/10.1002/aenm.201870034

Link

http://nrs.harvard.edu/urn-3:HUL.InstRepos:36305740

Terms of use

This article was downloaded from Harvard University’s DASH repository, and is made available under the terms and conditions applicable to Other Posted Material (LAA), as set forth at
https://harvardwiki.atlassian.net/wiki/external/NGY5NDE4ZjgzNTc5NDQzMGIzZWZhMGFlOWI2M2EwYTg

Accessibility

https://accessibility.huit.harvard.edu/digital-accessibility-policy

Share Your Story

The Harvard community has made this article openly available.
Please share how this access benefits you. Submit a story

WILEY-VCH

DOI: 10.1002/ ((please add manuscript number))

Article Type: Full Paper

Alkaline benzoquinone aqueous flow battery for large-scale storage of electrical energy

Zhengjin Yang†, Liuchuan Tong†, Daniel P. Tabor, Eugene S. Beh, Marc-Antoni Goulet, Diana De Porcellinis, Alán Aspuru-Guzik, Roy G. Gordon*, Michael J. Aziz*

Dr. Zhengjin Yang, Dr. Eugene S. Beh, Dr. Marc-Antoni Goulet, Dr. Diana De Porcellinis, Prof. Roy G Gordon, Prof. Michael J Aziz
Harvard John A. Paulson School of Engineering and Applied Sciences, 29 Oxford Street, Cambridge, Massachusetts 02138, USA
Email: maziz@harvard.edu (Michael J Aziz) gordon@chemistry.harvard.edu (Roy G Gordon)

Liuchuan Tong, Dr. Daniel P. Tabor, Dr. Eugene S. Beh, Prof. Alán Aspuru-Guzik, Prof. Roy G. Gordon
Department of Chemistry and Chemical Biology, Harvard University, 12 Oxford Street, Cambridge, Massachusetts 02138, USA

Dr. Zhengjin Yang
CAS Key Laboratory of Soft Matter Chemistry, *i*ChEM (Collaborative Innovation Center of Chemistry for Energy Materials), School of Chemistry and Material Science, University of Science and Technology of China, Hefei 230026, P.R. China

Dr. Eugene S. Beh
Current address: Palo Alto Research Center, 3333 Coyote Hill Road, Palo Alto, CA 94303

† These authors contributed equally.
*Corresponding authors:

Roy G. Gordon
Cabot Professor
Dept. of Chemistry and Chemical Biology
12 Oxford Street, MA 02138, USA
Tel: +1 617-495-4017
Fax: +1 617-495-4723
email: Gordon@chemistry.Harvard.edu

Michael J. Aziz
Gene and Tracy Sykes Professor of Materials and Energy Technologies
Harvard John A. Paulson School of Engineering and Applied Sciences, Pierce Hall 204a
29 Oxford Street, MA 02138, USA
Tel: +1 (617) 495-9884
email: maziz@harvard.edu

Key words: energy storage, alkaline aqueous flow battery, benzoquinone, molecular simulation

Abstract: We introduce an aqueous flow battery based on low-cost, non-flammable, non-corrosive and Earth-abundant elements. During charging, electrons are stored in a concentrated water solution of 2,5-dihydroxy-1,4-benzoquinone (DHBQ), which rapidly receives electrons with inexpensive carbon electrodes without the assistance of any metal electro-catalyst. Electrons are withdrawn from a second water solution of a food additive, potassium ferrocyanide ($K_4Fe(CN)_6$). When these two solutions flow along opposite sides of a cation-conducting membrane, this flow battery delivers a cell potential of 1.21 V, a peak galvanic power density of 300 mW/cm^2 and a coulombic efficiency exceeding 99%. Continuous cell cycling at 100 mA/cm^2 shows a capacity retention rate of 99.76%/cycle over 150 cycles. Various molecular modifications involving substitution for hydrogens on the aryl ring were implemented to block decomposition by nucleophilic attack of hydroxide ions in solution. These modifications resulted in increased capacity retention rates of up to 99.962%/cycle over 400 consecutive cycles, accompanied by changes in voltage, solubility, kinetics and cell resistance. Quantum chemistry calculations of a large number of organic compounds predicted a number of related structures that should have even higher performance and stability. Flow batteries based on alkaline-soluble dihydroxybenzoquinones and derivatives are promising candidates for large-scale, stationary-storage of electrical energy.

1. Introduction

The replacement of fossil-fuel energy with renewable sources has been increasing as the cost of solar and wind energy falls rapidly. Recent reports show that from 2008 to 2015, the cost of wind generation fell by 41%, rooftop solar photovoltaic installations by 54%, and utility-scale photovoltaic installations by 64%. The cost of solar panels now takes up less than 30% of a fully installed solar electricity system. [1] Although the cost of electricity from wind and sunlight has dropped dramatically, their widespread adoption is impeded by the inherent intermittency of these renewable energy sources. Safe, low cost, efficient, and scalable energy storage could solve this problem.

A number of energy storage options are available, such as pumped hydro, flywheels, compressed air, supercapacitors, solid-electrode batteries, and redox flow batteries (RFBs) [2]. In RFBs the redox-active species are separately stored in electrolytes in external tanks, and react reversibly in a device similar to a fuel cell when they are pumped past the electrodes (**Figure. 1**). This design offers significant advantage over solid electrode batteries, by decoupling energy and power output: the former is determined by the tank size and electrolyte concentration, the latter by electrode area [3]. Moreover, aqueous RFBs eliminate the safety issues posed by flammable organic solvents and, due to low electrolyte resistance, enable high current densities. The all-vanadium RFB, which has been the most heavily commercialized, is restricted by the low earth-abundance and the high and fluctuating cost of vanadium [4]. Aqueous organic redox flow batteries (AORFBs) exploiting water-soluble organic and organometallic redox-active molecules that are composed of only earth-abundant elements [5] have been the subject of recent research. AORFBs offer structural diversity, tunable redox potential and optimizable solubility [6]. High aqueous solubility, well-separated reduction potentials barely avoiding water splitting, stability, safety, and low cost at mass-production scales constitute the most critical attributes for novel aqueous organic electrolytes.

(insert Figure. 1)

Small molecule-based AORFBs can be run at acidic [5a], neutral [3a, 5e], or basic pH [5c, 5d, 7]. Substantially higher cell potentials have been demonstrated in basic pH. A current challenge for AORFBs is reaching high energy density (governed by the product of reactant

concentration and cell potential) while keeping reactant cost per kWh of energy storage capacity below the corresponding value for vanadium. Anthraquinone-2,7-disulfonate is a negative reactant with high solubility (2.8 M electrons) for an acidic RFB with cost per kWh roughly 1/3 that of vanadium but, when paired with a bromine/bromide positive reactant, delivers only a modest voltage of 0.81 V [5a](See also **Supplementary Table S1 and Figure.S1**). 2,6-dihydroxy-anthraquinone has comparable cost and is soluble in alkaline media (1.2 M electrons), where it has been demonstrated as a negative reactant in a 1.20-volt cell against $K_4Fe(CN)_6$ [5d]. Benzoquinones, which are substantially less expensive than anthraquinones (*vide infra*), have been utilized in acidic cells: 4,5-dihydroxybenzene-1,3-disulfonic acid [5f, 5g] and 3,6-dihydroxy-2,4-dimethylbenzenesulfonic acid [5h] have each been paired on the positive electrode with anthraquinone-2,6-disulfonic acid on the negative electrode. To date, these cells have been limited by low voltage, with discharge potential < 0.4 V when cycling stably. Here we report the performance of 2,5-dihydroxy-1,4-benzoquinone (DHBQ) as a promising negolyte (negative electrolyte) material for basic pH. DHBQ is highly soluble in base (> 8 M electrons in 1M KOH) with low reduction potential (-0.72 V vs. SHE at pH 14). Although mass production cost is hard to ascertain for new molecules, our investigation of lab-scale reagent grade prices from commercial vendors suggests DHBQ can be obtained at much lower prices than anthraquinones. (**Supplementary Table S1 and Figure. S1**). We paired DHBQ with potassium ferrocyanide to create an AORFB with a cell potential of 1.21 V. Cells exhibited peak power densities of up to 300 mW/cm^2, limited primarily by membrane resistivity, and capacity retention rates upon cycling of up to 99.76% per cycle over 150 cycles. The capacity loss of 0.24% per cycle appears to be caused by a combination of DHBQ crossover through the membrane and the chemical instability of DHBQ. Strategies were undertaken to further raise the capacity retention rate. By blocking the un-substituted carbon atoms in DHBQ, a hydroxylated benzoquinone–based AORFB was attained with improved stability, showing a capacity retention rate of 99.962% per cycle over 400 consecutive cycles, albeit with increased internal resistance.

The ultimate goal for organic flow battery reactants is to achieve sufficient stability at a

reasonable cost. For long-lifetime projects such as flow batteries for grid storage, discounting can become an important consideration. If the present value of the accumulated annual replacement cost is less than the savings in capital cost compared to vanadium then, other things being equal, the low-cost, shorter-lived reactant is the lower-cost option. This is illustrated in **Figure. 2**, which displays the breakeven point for the ratio of the annual replacement cost to the capital cost savings between a lower cost organic electrolyte and a higher cost infinitely stable reactant. For example, if the infinite-life electrolyte cost is 50$/kWh and the low-cost organic reactant costs 10$/kWh but requires 30% be replaced per year, the breakeven ratio is (30%*10)/ (50-10) = 7.5%. For a 20-year project, replacement of the cheaper shorter-lived reactant becomes the economically favorable choice when the interest rate for discounting exceeds 4%. This requires, of course, that decomposition products do not compromise the battery performance and that replacement is technically achievable and has negligible additional associated costs. We propose that benzoquinone functionalization, similar to the one presented in this study, is a promising path toward achieving this commercialization goal.

(insert Figure. 2)

2. Results and Discussion

2,5-dihydroxy-1,4-benzoquinone (DHBQ). DHBQ is ubiquitous in cellulose products and is the major survivor of bleaching treatment of cellulose products[8]. It is readily formed from the breakdown of cellulose products and enjoys high resistance towards oxidants such as hydrogen peroxide, ozone and oxygen by virtue of resonance stabilization[8] (**Figure.3**). The accumulation of negative charge at the unsubstituted positions mitigates possible attack by nucleophilic species (e.g. water or OH^-) through Michael addition, which was proposed to be the major mechanism of capacity fade in an AORFB with a 1,2-benzoquinone-3,5-disulfonic acid posolyte (positive electrolyte).[5g] The combination of chemical resistance and synthetic accessibility of DHBQ made it a logical alternative to investigate.

(insert Figure. 3)

Initial cyclic voltammetry experiments confirmed that DHBQ undergoes reversible

two-electron reduction/oxidation, with well-defined anodic and cathodic peaks having a small peak separation (**Supplementary Figure.S2**). In order for DHBQ to be used in a practical cell, it has to have a high solubility at the operating pH. As expected, DHBQ is highly soluble at high pH due to its two solubility-enhancing hydroxy groups, which are deprotonated above pH 10. UV-Vis spectrophotometry of a saturated solution of DHBQ potassium salt in 1 M KOH showed a solubility of 4.31 M (**Supplementary Figure.S3**), which corresponds to an negolyte (negative electrolyte) capacity of 231 Ah/L. A comparison of DHBQ with other reported AORFB negolytes (**Supplementary Table S1**) shows that DHBQ enjoys high commercial availability, high solubility, low cost and low redox potential.

Effect of pH on DHBQ redox behavior. DHBQ behaves differently from other quinones, such as DHAQ[5d]. DHBQ exhibits well-defined anodic and cathodic peaks at pH values of 4 or lower and of 12 or higher (**Figure.4, Supplementary Table S2 and Figure.S2**), but not in between. At the lowest pH value investigated (0.0, from 1M H_2SO_4), DHBQ shows well-defined and reversible oxidation and reduction peaks, characterized by a redox potential of 0.41V vs. SHE with an anodic-cathodic peak separation of 40 mV. Increasing the solution pH lowers the redox potential and increases the peak separation, as shown in Fig. 4, indicating the transition from a reversible reaction to a quasi-reversible reaction. The average slope of the redox potential vs. pH over the pH range 0-3.28 is -66±2 mV per pH unit, which is close to the value of -59 mV/pH expected from a two-electron, two-proton process. The absolute magnitudes of the peak heights are also consistent with a two-electron process. In the intermediate pH range, we did not observe any electrochemically reversible behavior of DHBQ, with either no oxidation signal or no reduction signal seen upon cycling. Above pH ~11.8, a quasi-reversible redox reaction reemerges, with redox potential of -0.67 V vs. SHE and peak separation of 69 mV. When the pH is further increased to 14 (1 M KOH), well-defined reversible oxidation and reduction peaks were again observed, with a redox potential of -0.72 V and a peak separation of 58 mV.

(insert Figure. 4)

Redox kinetics of DHBQ. We performed rotating-disk-electrode experiments to evaluate the reduction kinetics of DHBQ, by sweeping negatively from -0.3 V to -1.4 V vs. SHE. Voltammograms were acquired over a range of rotation rates (**Figure.5**). A diffusion coefficient (*D*) of 3.66×10^{-6} cm^2/s was determined from a Levich plot of the limiting current vs. square root of rotation rate. A Koutecký-Levich plot reveals good linearity of reciprocal electrode currents against the reciprocal square root of rotation rate at different overpotentials from the formal reduction potential (E^0 = -0.72 V vs. SHE at pH 14). Fitting the kinetically-limited current i_k to the Tafel equation yields an electron transfer rate constant (k^o) of 2.12×10^{-3} cm/s. Compared with other small redox-active molecules, DHBQ shows a diffusion coefficient similar to those of 9,10-anthraquinone-2,7-disulphonic acid [5a], ferrocene derivatives[3a], TEMPO derivatives or viologens[9], and slightly higher than those of the sodium salts of flavin mononucleotide[7] and DHAQ[5d]. As expected, the experimental diffusion coefficient is 5 orders of magnitude higher than that of the redox-active polymers that have been demonstrated in an aqueous RFB[5b]. The electron-transfer rate constant (k^o) is greater than those of ferrocene derivatives[3a], alloxazine [5c], V^{3+}/V^{2+} and VO^{2+}/VO_2^+ [10], which makes it promising as an AORFB reactant (**Supplementary Table S3**).

(insert Figure. 5)

DHBQ/$K_4Fe(CN)_6$ alkaline AORFB. To demonstrate the capability of DHBQ as the negolyte for an alkaline AORFB, a lab-scale AORFB prototype was assembled using graphite flow plates with serpentine flow fields (**see details in supplementary information**). The positive reservoir (6 mL) comprised 0.4 M potassium ferrocyanide ($K_4Fe(CN)_6$) in 1 M KOH and the negative reservoir (22.5 mL) was assembled from 0.5 M of DHBQ in 2 M KOH (1 M OH^- was consumed in deprotonating DHBQ). A lower DHBQ concentration than the solubility limit was utilized to ensure osmotic balance with the ferrocyanide posolyte, which has a limited solubility in 1M KOH. The theoretical cell potential of DHBQ/$K_4Fe(CN)_6$in 1 M KOH is 1.21 V(**Figure.1**). We varied the state of charge (SOC) by a constant-coulomb incremental charging technique from 10% to ~100% and recorded the corresponding open-circuit voltage (**Supplementary Figure.S4**). The cell potential at 10% SOC is 1.141 V

and climbs up to 1.202 V at 50% SOC. The cell voltage reaches 1.255 V at ~100% SOC.

Initial cell performance was evaluated with three different commercial cation exchange membranes, namely Nafion 212 (N212), Nafion 115 (N115) and Nafion 117 (N117). Polarization curves (**Figure. 6**) show that the cells assembled with N212, N115 and N117 exhibit peak power densities of 300 mW/cm^2, 164 mW/cm^2 and 137 mW/cm^2, respectively. The difference in peak power density results from the overall cell resistance as reflected in the potential-current curves. The direct current area-specific resistance (DC-ASR) was obtained as the derivative of the potential vs. current density curve at open-circuit voltage (OCV). The DC-ASR of the DHBQ/$K_4Fe(CN)_6$ cells with N212, N115 or N117 membranes was 1.28 Ω cm^2, 2.41 Ω cm^2 and 2.85 Ω cm^2, respectively. Electrochemical impedance spectroscopy (EIS) measurements indicate that the membrane resistance is responsible for > 85% of the DC-ASR (**Supplementary Figure.S5**).

(insert Figure. 6)

DHBQ/$K_4Fe(CN)_6$ cell cycling. Cell cycling experiments were conducted to evaluate the capacity retention rate of the DHBQ/$K_4Fe(CN)_6$ cell. Prior to cycling, the cell capacity was evaluated with a full charge-discharge process to be 531.4 C, which is 91.8% of the theoretical value (578.9 C in 6 mL negolyte). When cycled galvanostatically at 100 mA/cm^2 between voltage cutoffs of 1.6 and 0.6 V, the initial capacity was 23.15 Ah/L, which is 86.4% of the theoretical capacity, 26.79 Ah/L. We tentatively attribute the value of 91.8% to DHBQ purity and transfer loss, the difference between 91.8% and 86.4% to overpotential during cell cycling. The DHBQ/$K_4Fe(CN)_6$ cell assembled with the N212 membrane suffers from severe capacity fade (**Supplementary Figure. S6**). The coulombic efficiency (CE), which is the ratio of the discharge capacity to the immediately preceding charge capacity, is around 77% and drops to 72.5% after 10 cycles. The low value of the CE indicates that self-discharge of the N212-cell is taking place during cycling, which we hypothesize to be caused by crossover of active electrolytes across the membrane. The high DHBQ crossover rate stems from its small molecular size as well as the high water-uptake and small thickness of N212 membrane (**Supplementary Table S4**). On the one hand, by switching to thicker membranes, N115 and N117 (**Figure. 7, Supplementary Fig.S7**), a clear increase in the coulombic efficiency of the

cell of up to 99% is observed. This coulombic efficiency remains high during cycling, suggesting a reduced membrane crossover rate of the capacity-limiting reagent, DHBQ. The same capacity is obtained at 100 mA/cm^2 with either the N115 or the N117 membrane, but not with N212. On the other hand, thicker membranes contribute a higher area-specific resistance, as reflected in the polarization curves (**Figure.6**); high resistance in turn leads to decreased round-trip energy efficiency (EE). The EE of N117-based DHBQ/$K_4Fe(CN)_6$ cell is around 61% at first and stabilizes at ~ 56%, whereas it is slightly higher for a N115-based DHBQ/$K_4Fe(CN)_6$ cell and remains comparatively stable at 65%. If the current efficiency loss current is independent of current density, then the EE of the N115 cell can be increased to ~88% by reducing the current density to 15 mA/cm^2 – but at an increased capital cost per kW due to the large cell area per unit current.

The capacity retention rates for N115-based and N117-based cells are 99.76% and 99.68% per cycle, respectively. Although the cell remains quite stable from each charge-discharge cycle to the next, the accumulation of the tiny capacity fade during prolonged cycling is not ideal for practical application. The capacity fade rate for the N115-based cell of 0.24% per cycle extrapolates, assuming exponential decay, to 290 cycles before the capacity drops to 50% of the original, which is inadequate for practical application.

(insert Figure. 7)

Capacity · retention analysis. By reducing the volume of the positive reservoir, a DHBQ/$K_4Fe(CN)_6$ cell that was capacity-limited by the posolyte was assembled and cycled. Results (**Supplementary Figure.S8**) show that discharge capacity of the cell remained unchanged for the first 45 cycles (around 20 hours), although the charge-capacity varied slightly. This implies that $K_4Fe(CN)_6$ loss is not contributing to the capacity loss of the DHBQ/$K_4Fe(CN)_6$ cell.

The crossover rate of DHBQ across a N115 membrane was measured in a two-compartment rotating cell (**see permeability measurements in Supplementary Information for details**). The DHBQ concentration in the receiving reservoir was found to

increase linearly over time, indicating a permeability of $1.27*10^{-9}$ cm^2/s (**Supplementary Figure. S9**). Considering the time every cycle takes, the effective membrane area and the reservoir volume of the cell, the expected capacity loss caused by DHBQ crossover would be 0.012% per cycle. Although the membrane properties in a static permeability measurement may not permit one to accurately infer its properties in a cycling cell, this is more than an order of magnitude below the observed capacity loss rate in a cycling N115-based DHBQ/$K_4Fe(CN)_6$ cell (0.24% per cycle). The discrepancy suggests molecular decomposition as a potential mechanism of capacity fade. This hypothesis was then tested by separate experiments, in which the negolyte solution composition after cell cycling, and DHBQ stored in alkaline solutions at elevated temperature, were both analyzed using NMR. A typical ^{1}H-NMR spectrum (**Supplementary Figure.S10**) was too complicated to interpret and suggests the coexistence of multiple species. However, more information was extracted from the ^{13}C-NMR spectra (**Supplementary Figure.S11**). According to the standard spectra of DHBQ in DMSO-d_6 provided by Sigma-Aldrich, two carbon signals should be observed, one at 105 ppm and the other at around 172 ppm; however, the latter is broad and could hardly be observed. After 300 cell cycles, a new peak was observed at 162 ppm, indicating the generation of a new species during cycling. Combined with the information obtained from the ^{1}H-NMR spectrum, we conclude that multiple species are generated during cell cycling although their concentrations are not high enough to be clearly observed in the ^{13}C-NMR spectra. In a separate experiment, in which the oxidized form of DHBQ was subjected to prolonged ex-situ alkaline treatment at an extremely elevated temperature of 80 °C for 40 days, no carbon peaks at all could be observed, indicating that DHBQ had degraded chemically. LC-MS analysis of a fresh DHBQ solution shows a single peak at a retention time of 14–15 min, with a mass(m/z) of 139.0037, which agrees exactly with the chemical structure. Although DHBQ could be detected in the LC-MS spectrum of the alkaline treated DHBQ solution, multiple peaks were observed, which is consistent with the results we obtained in NMR study (**Supplementary Figure.S12 and S13**). Despite the fact that LC-MS was able to detect the mass of each peak, we have not yet determined the degradation mechanism. Our working hypothesis is that the chemical decomposition of DHBQ during cell

cycling is possibly caused by nucleophilic attack of the hydroxide ions on the un-substituted carbon atoms of DHBQ.

Capacity retention rate enhancement. Based on the suspected chemical decomposition mechanism of DHBQ, strategies were then taken to further increase the capacity retention rate of a DHBQ/$K_4Fe(CN)_6$ cell by decreasing the hydroxide concentration in the supporting electrolyte and by blocking the un-substituted positions in the benzoquinone ring. A DHBQ/$K_4Fe(CN)_6$ cell was run at pH 12 (0.01 M KOH), at which DHBQ still exhibits well-defined reversible oxidation and reduction peaks (**Supplementary Figure.S2**) despite its reduced solubility (around 0.3 M electrons, **Supplementary Figure.S3**) compared to at pH 14. The cell potential remains close to that of the cell run at pH 14. Galvanostatic charge-discharge cycling was conducted at 40 mA/cm^2 and the evolution of the overall cell capacity was evaluated by fully charging and then fully discharging the cell once every 10 cycles (**Supplementary Figure.S14**). The overall discharge capacity retention rate was 99.98% per cycle, which extrapolates, assuming exponential decay, to over 3,400 cycles before the capacity decays to 50% of its initial value. The results confirm the effectiveness of enhancing capacity retention of DHBQ/$K_4Fe(CN)_6$ cell at lower OH^- concentration.

It has been proposed that the degradation of benzoquinones in acidic conditions is caused by Michael addition[5g], which can be mitigated by a blocking strategy[5h]. In basic pH, hydroxide ions are stronger nucleophiles than is water in acid. Synthetic efforts were made to verify the effectiveness of improving the chemical stability of DHBQ by blocking the un-substituted positions. 3,6-bis(diphenylmethyl)-2,5-dihydroxy-1,4-benzoquinone (DPM-DHBQ) was synthesized using a reported procedure and characterized by cyclic voltammetry (**see Supplementary Information for details**). Results indicate that DPM-DHBQ is redox-active and the reduction and oxidation occur at -1.0 V and -0.5 V, respectively, showing a half-wave potential of roughly -0.75 V vs. SHE (**Supplementary Figure.S15**). The redox potential is close to that of DHBQ, and the peaks remain unchanged during repeated scans. However, adding extra aromatic rings to block the un-substituted carbon atoms led to an increased peak separation in the CV, implying sluggish redox kinetics on glassy carbon. Incorporating extra aromatic rings also caused a severe decrease in

solubility that precluded full cell studies. Considering the acquired facts and synthetic difficulties, molecular simulations were conducted to help understand the behavior of blocked-DHBQ molecules and are presented in a later section.

Alternatively, the vulnerable 3- and 6- positions on DHBQ can also be blocked by polymerization. The polymerization of benzoquinone in alkaline solutions (polyBQ, **see Supplementary Information for details**) and the acid-catalyzed condensation of DHBQ with formaldehyde[11] generate polymers that have repeating units with a similar structure to DHBQ. Furthermore, we anticipate such structures would be redox-active but no longer susceptible to nucleophilic attack.

(insert Figure. 8)

A polyBQ/$K_3Fe(CN)_6$ cell was assembled and run at pH 14 (Potassium ferricyanide, $K_3Fe(CN)_6$ was utilized because polyBQ is produced in its reduced form.). Similarly, the constant-coulomb incremental charging technique was utilized and the open-circuit voltage at 10% SOC is 0.806 V, which increases to 1.279 V at ~100% SOC (**Supplementary Figure. S16**). The potential at 50% SOC, 1.004 V, is lower than that of the DHBQ/$K_4Fe(CN)_6$ cell. Polarization curves (**Supplementary Figure.S17**) show that the peak power density of the polyBQ/$K_3Fe(CN)_6$ cell at ~100% SOC is approximately 30 mW/cm^2. The low peak power density is because of the extremely high overall resistance (DC-ASR), which is over 9 Ωcm^2; the resistance is four times that of the DHBQ/$K_4Fe(CN)_6$ cell with the same membrane. *In-situ* EIS measurements showed that the high-frequency resistance of the cell (**Supplementary Figure.S18**) was more than doubled by the replacement of DHBQ with polyBQ. Based on our established resistance model [12], the high-frequency resistance is dominated by the membrane resistance, which may have suffered increases due to the plugging of ionic transport channels by polyBQ. It is also possible that polymerization has reduced the ionic diffusivity in the electrolyte to the point that mass transfer limitations have become important.

The assembled polyBQ/$K_3Fe(CN)_6$ cell was cycled for 400 cycles at 10 mA/cm^2 (**Figure.8**). The CE and EE at 10 mA/cm^2 were 96% and 37%, respectively and remained unchanged over 400 cycles, indicating a stable charge-discharge process. The capacity of the

cell is ~25 % of the theoretical capacity, which may be due to the coil-conformation and chain entanglement of polyBQ in solution, as well as the slower kinetics compared with small molecules. In the meantime, the increase in viscosity due to increased molecular size also reduces the contact of redox-active repeating units to the electrodes. During the first 100 cycles, the capacity is slightly variable and increases slightly. During the following 300 cycles, the capacity retention rate was 99.962%/cycle (**Figure. 8a**). Compared with the highest capacity retention rate we acquired for a N115-based DHBQ/$K_4Fe(CN)_6$ cell (99.76% per cycle), the improvement in capacity retention rate supports our hypothesis about the effectiveness of the blocking strategy. We believe further increase in capacity retention rate can be achieved by incorporating poly(2,5-dihydroxyl-1,4-benzoquinone-3,6-methylene), the polymer from acid-catalyzed condensation of DHBQ with formaldehyde (**Supplementary Figure. S19**), as negolyte. Although the reaction was claimed to be readily carried out [11], we have encountered more difficulties than expected in acquiring the polymeric products. Future research effort will focus on understanding the difference in redox behavior between the monomer and its polymer counterpart. Synthetic efforts will also be devoted to acquiring the most promising substituted DHBQ based on theoretical modelling and evaluating the electrochemical properties.

Theoretical modelling and screening. Given the promise of DHBQ, we conducted a virtual screening of modified DHBQ molecules to identify potential improvements, understand potential effects of polymerization at the monomer level, and gain insights about the chemical space in the vicinity of the molecule. For this work, two properties were considered, the first being the reduction potential vs. DHBQ and the second being the redox behavior. Molecules that exhibit a one-step $2e^-$ oxidation/reduction behavior in computed processes are favored, because reactive radical intermediates might be generated during a two-step sequence of $1e^-$ oxidation/reduction processes. Thus, we seek to minimize the overall two-electron reduction potential (without promoting conditions that evolve H_2), while also maintaining the one-step $2e^-$ oxidation/reduction in simulation and maximize solubility. A full list of the results for the screened molecules can be found in the supplementary information (**Supplementary Table S5 and Table S6, Supplementary Figure. S20-S22**); in **Table 1** we

report the most promising molecules. The molecules in **Table 1** satisfy the following criteria: a cell voltage more than 0.1 V higher than that of DHBQ when paired with ferrocyanide (i.e. a reduction potential more than 0.1 V lower than DHAQ), a predicted solubility of > 1 M (LogS > 0), and predicted to be a one-step reduction.

Here we discuss some illustrative cases. First, DHBQ derivatives with alkyl substitutions were explored to elucidate the differences in the reduction potential between the subunits of polymers and the DHBQ monomer. In general, in the addition of shorter alkyl chains reduces the reduction potential relative to DHBQ, though there are some instances in Table S6 where alkyl substitutions on DHBQ would lower the cell potential. From the group with shorter alkyl chain substitutions, the molecule in **Table 1** with two $CH_2N(CH_3)_2$ substitutions is predicted to have the highest cell voltage. (see supplementary Tables S5 and S6 for a list of some of the compounds considered).

Second, we considered modifications of the OH groups on DHBQ (in conjunction with the other substitutions), including substituting them with polyether chains. Interestingly, the substitution of a single polyethylene glycol subunit typically decreases the cell voltage relative to DHBQ, whereas the replacement of OH by a two-or three-unit polyethylene glycol chain increases the cell voltage. We also examined the substitution of the non-OH sites with similar chains and found that when combining two OH groups with a pair of three ethylene glycol chain substitutions, the cell voltage is predicted to be 0.21 V higher than that of DHBQ. Based on this and the predicted solubility in basic solution, this molecule appears to be one of the most promising in this group.

(insert Table. 1)

3. Conclusions.

Our results indicate that DHBQ-based reactants are promising for alkaline organic RFBs. Compared with anthraquinone-based reactants, benzoquinones have higher alkaline solubility, lower molecular weight, and lower cost. The lower molecular weight, however, causes enhanced membrane permeability and thereby poses challenges for membrane development

toward low molecular permeability while maintaining high ionic conductivity, in order to prevent capacity fade due to molecular crossover. Fortunately, many membranes now available seem to be sufficiently stable up to pH 14. 2,5-DHBQ, without further substitution, is not sufficiently stable to provide the service life needed for practical implementation. Our observations support the hypothesis that nucleophilic attack of hydroxide ions on the unsubstituted carbon atoms of the DHBQ aryl ring is responsible for the observed capacity fade. Synthesized derivatives of DHBQ, in which the aryl ring is fully substituted in various ways, substantially altered the capacity retention rate as well as the solubility and redox activity. The insight gained from computational screening, in conjunction with these experiments, points out avenues for further performance improvement and give us a fighting chance of using benzoquinone-based alkaline organic RFBs to provide safe, cost-effective, robust stationary electrical energy storage.

Supporting Information

Supporting Information is available from the Wiley Online Library or from the author.

Acknowledgements.

Dr. Zhengjin Yang greatly appreciates financial support from the National Science Foundation of China (No. 21506201) and a scholarship from the China Scholarship Council to study at Harvard University. The work was supported in part by the following organizations: the U.S. Department of Energy contract DE-AC05-76RL01830 through PNNL subcontract 304500; ARPA-E award DE-AR0000348; the Harvard School of Engineering and Applied Sciences and the Massachusetts Clean Energy Technology Center. The authors thank Dr. Michael R Gerhardt, Dr. David Kwabi and Andrew Wong for assistance and helpful discussions on experimental electrochemical techniques.

References

[1] a) B. Obama, *Science* **2017**, 355, 126; b) N. S. Lewis, *Science* **2016**, 351, aad1920.

[2] a) J. Winsberg, T. Hagemann, T. Janoschka, M. D. Hager, U. S. Schubert, *Angew. Chem. Int. Ed. Engl.* **2017**, 56, 686; b) P. Alotto, M. Guarnieri, F. Moro, *Renewable*

Sustainable Energy Rev. **2014**, 29, 325.

[3] a) B. Hu, C. DeBruler, Z. Rhodes, T. L. Liu, *J. Am. Chem. Soc.* **2017**, 139, 1207; b) T. Liu, X. Wei, Z. Nie, V. Sprenkle, W. Wang, *Adv. Energy Mater.* **2016**, 6, 1501449; c) M. Park, J. Ryu, W. Wang, J. Cho, *Nat. Rev. Mater.* **2016**, 2, 16080.

[4] a) C. J. Barnhart, S. M. Benson, *Energy Environ. Sci.* **2013**, 6, 1083; b) M. Armand, J. M. Tarascon, *Nature* **2008**, 451, 652.

[5] a) B. Huskinson, M. P. Marshak, C. Suh, S. Er, M. R. Gerhardt, C. J. Galvin, X. Chen, A. Aspuru-Guzik, R. G. Gordon, M. J. Aziz, *Nature* **2014**, 505, 195; b) T. Janoschka, N. Martin, U. Martin, C. Friebe, S. Morgenstern, H. Hiller, M. D. Hager, U. S. Schubert, *Nature* **2015**, 527, 78; c) K. Lin, R. Gómez-Bombarelli, E. S. Beh, L. Tong, Q. Chen, A. Valle, A. Aspuru-Guzik, M. J. Aziz, R. G. Gordon, *Nature Energy* **2016**, 1, 16102; d) K. Lin, Q. Chen, M. R. Gerhardt, L. Tong, S. B. Kim, L. Eisenach, A. W. Valle, D. Hardee, R. G. Gordon, M. J. Aziz, M. P. Marshak, *Science* **2015**, 349, 1529; e) E. S. Beh, D. De Porcellinis, R. L. Gracia, K. T. Xia, R. G. Gordon, M. J. Aziz, *ACS Energy Letters* **2017**, 2, 639; f) B. Yang, L. Hoober-Burkhardt, F. Wang, G. S. Prakash, S. Narayanan, *J. Electrochem. Soc.* **2014**, 161, A1371; g) B. Yang, L. Hoober-Burkhardt, S. Krishnamoorthy, A. Murali, G. S. Prakash, S. Narayanan, *J. Electrochem. Soc.* **2016**, 163, A1442; h) L. Hoober-Burkhardt, S. Krishnamoorthy, B. Yang, A. Murali, A. Nirmalchandar, G. K. S. Prakash, S. R. Narayanan, *J. Electrochem. Soc.* **2017**, 164, A600.

[6] S. Er, C. Suh, M. P. Marshak, A. Aspuru-Guzik, *Chem. Sci.* **2015**, 6, 885.

[7] A. Orita, M. G. Verde, M. Sakai, Y. S. Meng, *Nat Commun* **2016**, 7, 13230.

[8] T. Hosoya, A. French, T. Rosenau, *Mini-Rev. Org. Chem.* **2013**, 10, 309.

[9] T. Janoschka, N. Martin, M. D. Hager, U. S. Schubert, *Angew. Chem. Int. Ed. Engl.* **2016**, 55, 14427.

[10] T. Yamamura, N. Watanabe, T. Yano, Y. Shiokawa, *J. Electrochem. Soc.* **2005**, 152, A830.

[11] T. Le Gall, K. H. Reiman, M. C. Grossel, J. R. Owen, *J. Power Sources* **2003**, 119-121, 316.

[12] Q. Chen, L. Eisenach, M. J. Aziz, *J. Electrochem. Soc.* **2015**, 163, A5057.

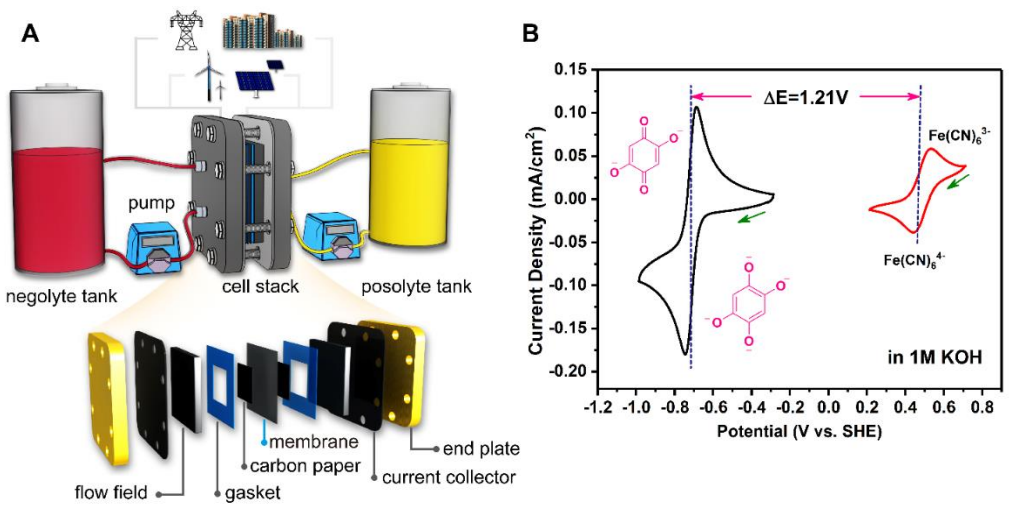

Figure. 1 (A) Illustration of the AORFB assembled in this contribution. The exploded scheme shows the components of the cell stack. (B) Cyclic voltammograms of 1mM potassium ferricyanide/ferrocyanide posolyte ($K_3Fe(CN)_6/K_4Fe(CN)_6$, red line) and 1mM DHBQ/reduced-DHBQ negolyte (black line) in 1 M KOH at a scan rate of 10 mV/s. Potentials are referenced to the standard hydrogen electrode (SHE). The theoretical cell potential is determined from the difference in reduction potentials (ΔE) of the posolyte and negolyte.

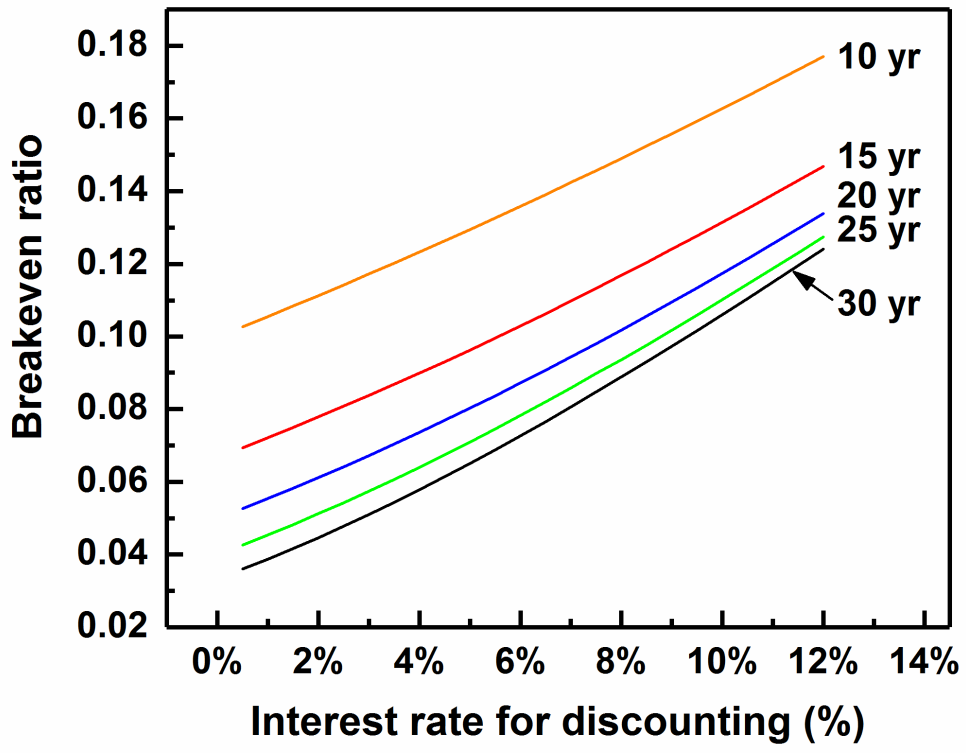

Figure. 2. Breakeven ratio of annual replacement cost to savings in capital cost vs. interest rate for discounting. A 10 to 30-year project life is assumed.

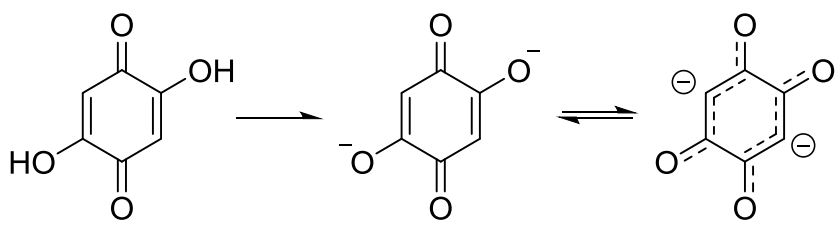

Figure. 3. DHBQ and its resonance stabilized dianions.

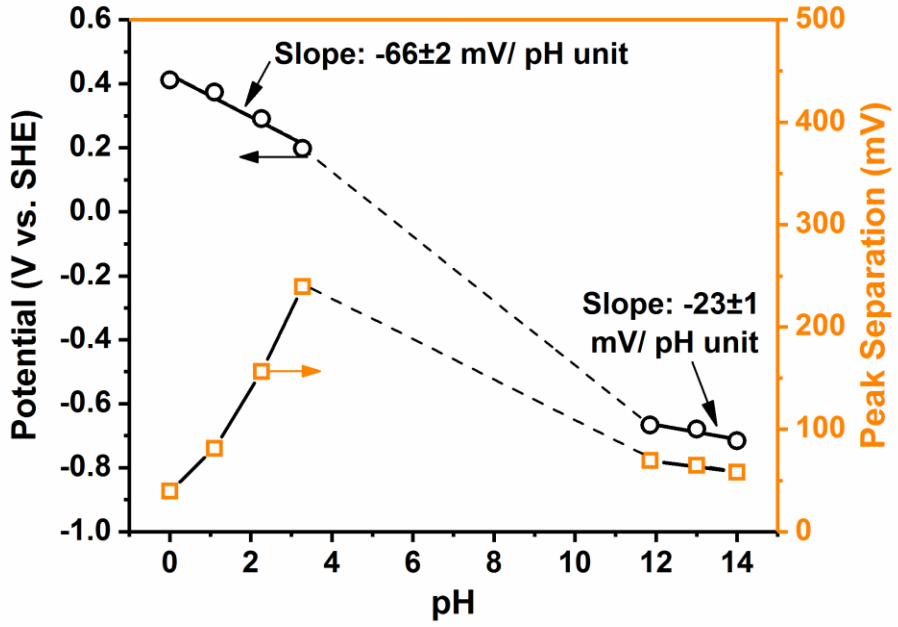

Figure. 4. Redox potential and anodic-cathodic peak separation of DHBQ as a function of pH

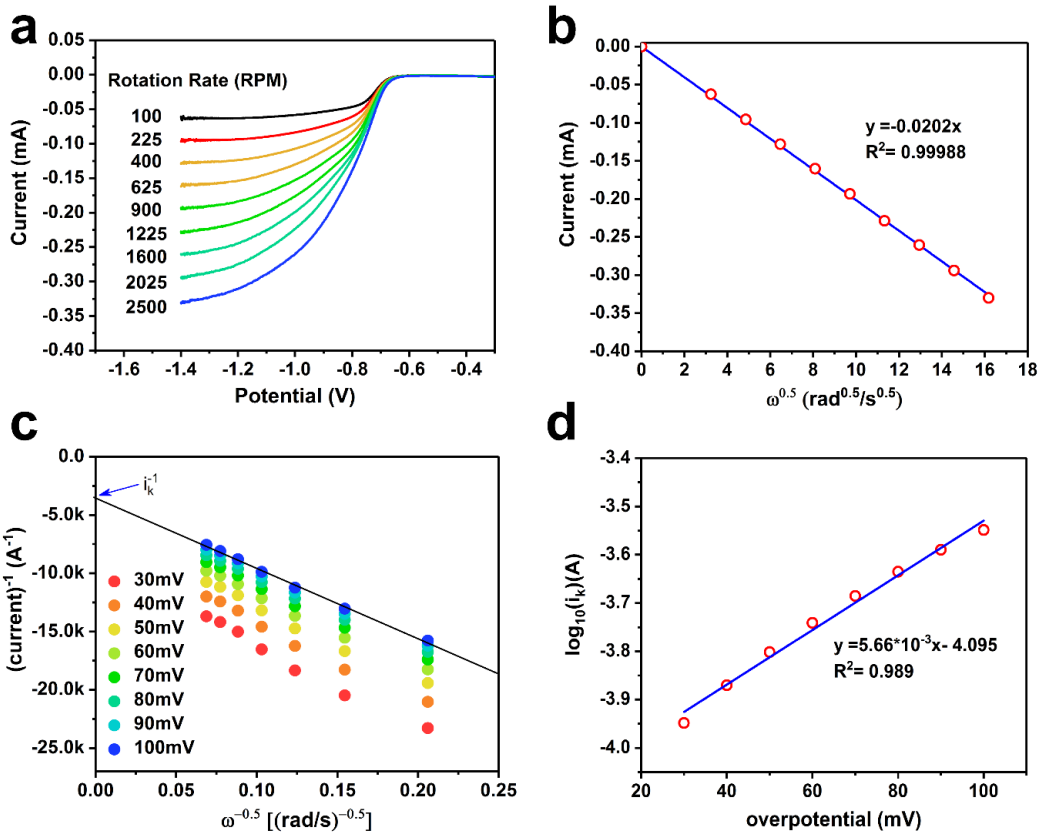

Figure. 5. Rotating-disk-electrode (RDE) experiment on DHBQ (1 mM in 1 M KOH). (a) Current versus potential at rotation rate from 100 rpm to 2500 rpm with potential sweep rate of 5 mV/s; (b) Levich-plot of limiting current versus square root of rotation rate ($\omega^{1/2}$); (c) Koutecky-Levich plot at different over-potentials; reciprocal of kinetically limited current is indicated on vertical axis. (d) Tafel plot, the logarithm of kinetically-limited current vs. overpotential (potential deviation from the formal reduction potential).

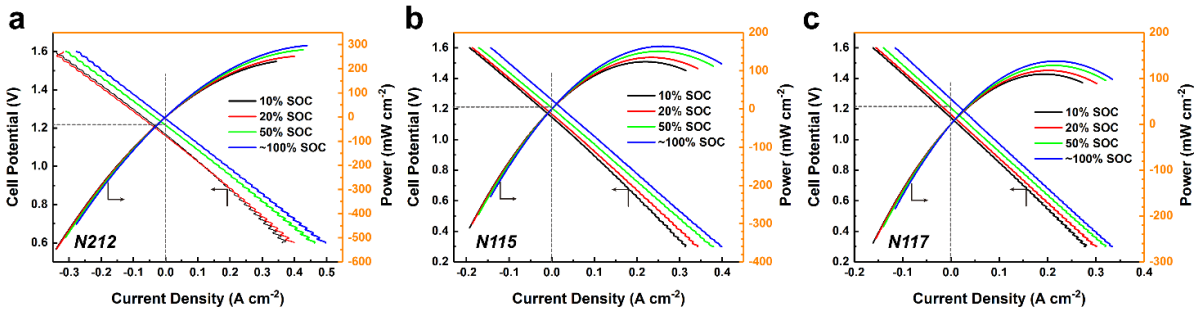

Figure. 6 Electrochemical performance of a DHBQ/$K_4Fe(CN)_6$ cell. Electrolytes comprise 6 mL of 0.5 M DHBQ in 2M KOH (the negolyte) and 22.5 mL of 0.4 M potassium ferrocyanide ($K_4Fe(CN)_6$) in 1M KOH (the posolyte). The cell-polarization plots, composed of cell potential (left vertical) and power density (right vertical) versus discharge current density, correspond to the cell assembled with (a) Nafion 212 membrane (N212), (b) Nafion 115 membrane (N115) and (c) Nafion 117 membrane (N117). The dashed lines indicate open circuit potential at 50% SOC.

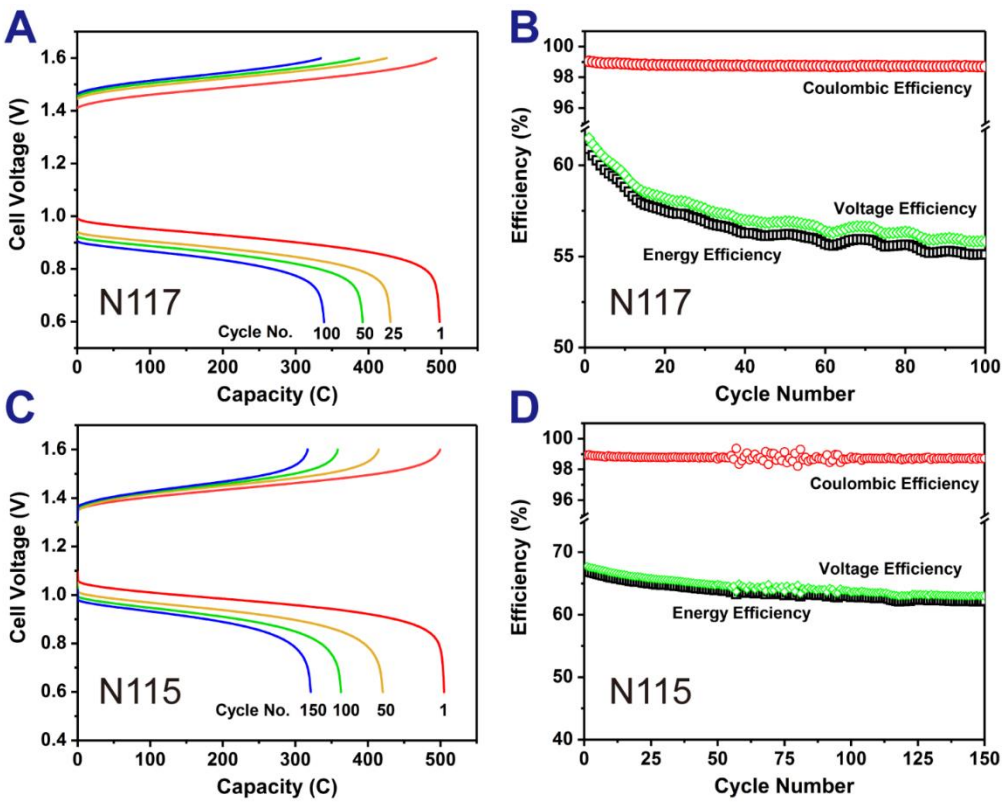

Figure. 7 Prolonged galvanostatic cell cycling performance of Nafion-based DHBQ/$K_4Fe(CN)_6$ cell at 100 mA/cm^2 with potential cut-offs of 1.6V and 0.6 V. No potential holds were employed. The electrolytes comprise 6 mL of 0.5 M DHBQ in 2 M KOH and 22.5 mL of 0.4 M $K_4Fe(CN)_6$ in 1 M KOH. Representative cell potential versus capacity curves (A and B for Nafion 117 membrane, C and D for Nafion 115 membrane) and efficiencies (coulombic efficiency, energy efficiency and voltage efficiency) over the whole cycling process are presented.

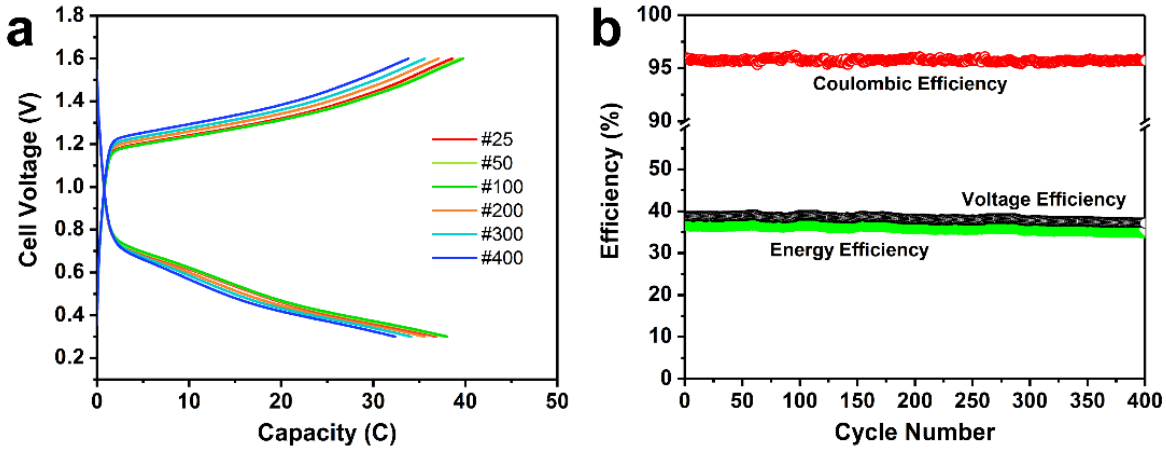

Figure. 8 Cell cycling performance of a polyBQ/ $K_3Fe(CN)_6$ cell utilizing Nafion 115. Due to a higher overall resistance, the cell was cycled at 10 mA/cm^2 with potential cut-offs of 1.6 V and 0.6 V, without any potential holds. Representative cell potential versus capacity curves (a) and efficiencies (b) over 400 consecutive cycles are presented.

Table 1. Calculated Reduction Potentials for Most Promising DHBQ Derivatives

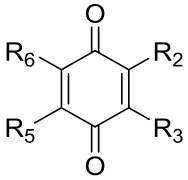

R_2, R_5	R_3, R_6	Predicted 2e Reduction Potential[a] (V)	Predicted Oxidized Form LogS at pH=14[b]
-OH	$-CH_2N(CH_3)_2$	-0.25	1.91
-OH	$-(CH_2OCH_2)_3$-OH	-0.21	2.65
-OH	$-CH_2NH_2$	-0.18	2.28
-OH	$-(CH_2CH_2O)_3$-H	-0.15	2.56
-OH	$-CH_2CH_3$	-0.15	0.14
$-(O-CH_2CH_2)_2$-OH	$-CH_2NH_2$	-0.14	0.08
-OH	$-CH_2CH_2NH_2$	-0.14	2.45
-OH	$-CH_3$	-0.12	1.49
$-(O-CH_2CH_2)_2$-OH	$-CH_2CH_2NH_2$	-0.12	0.30

[a] Calculated vs. DHBQ using B3LYP/6-311+G(d,p) CPCM

[b] Calculated using ChemAxon suite

Redox-active and cheap benzoquinone materials that store energy in considerably smaller volumes are reported. When paired with potassium ferrocyanide, an inexpensive and safe food additive, this flow battery chemistry delivers a cell potential of 1.21V and a peak galvanic power density of 300 mW/cm^2. Quantum computational simulation has also identified promising compounds for future improvements.

Keyword: energy storage, alkaline aqueous flow battery, benzoquinone, molecular simulation

Zhengjin Yang†, Liuchuan Tong†, Daniel P. Tabor, Eugene S. Beh, Marc-Antoni Goulet, Diana De Porcellinis, Alán Aspuru-Guzik, Roy G. Gordon*, Michael J. Aziz*
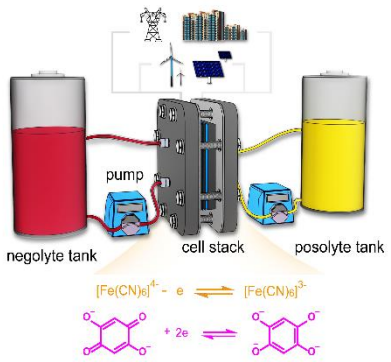
Alkaline benzoquinone aqueous flow battery for large-scale storage of electrical energy